Implementation of Innovative Measurement Technique for Precise Experimental Characterization of Frost Growth in a Heat Pump Evaporator

Antoine PARTHOENS[1*],Samuel GENDEBIEN[1], Vincent LEMORT[1]

[1] University of Liège, Aerospace & Mechanical Department, Thermodynamics Laboratory, Liège, Belgium
+32(0)4-366.48.16
a.parthoens@uliege.be

* Corresponding Author

ABSTRACT

Refrigeration systems such as heat pumps may be subject to frost formation due to ambient air humidity. This phenomenon plays a major role in the HP overall performance drop due to the presence of an additional thermal resistance and an increase of the air-side pressure drop.

The aim of this paper is to present a new innovative experimental technique to measure the amount of frost (or condensates) within the evaporator and therefore the air latent load. As the refrigerant distribution may vary with the frost apparition at the evaporator level, the exchanger cannot be weighted on its own to measure the frost mass over time. One of the main interesting features of the test rig consists in monitoring the weight of the heat pump as a whole. As the relative mass of the frost compared to the test rig is rather negligible, a counterweight has been designed to decrease the total load of the force sensor and therefore to increase the measurement accuracy dedicated to the frost mass measurement. The system is more elaborated and complex to set-up, but it brings much more confidant measurements on the mass, compared to a enthalpy balance based on humidity sensors. Mainly because it relies on only one sensor and there is no error propagation throughout the test.

The first phase of the experimental campaign specifically focuses on characterizing the evaporator behavior (without coating) under frosting conditions. As superhydrophobic coatings might represent an efficient solution to delay the frost formation, a second testing phase (not presented in this paper) will take place in order to characterize such coated evaporators and compare them to the bare ones.

The testing of different evaporators (coated and uncoated) will mark a fundamental contribution to the progress of understanding coated heat exchangers' behavior under frosting conditions. Lastly, the creation of the experimental database will feed the calibration of numerical models.

1. INTRODUCTION

Heat pumps are thermal systems allowing to heat up buildings in an environmentally friendly way. They draw the calories from several different heat sources, such as ground (geothermal), water or air. The air-source heat pumps are currently the more largely used.

The refrigerant running in the evaporator of the heat pump is generally at a very low temperature, below 0°C (Xu et al., 2019). In this context the humidity present in the air may desublimate (Piucco, Hermes, Melo, & Barbosa Jr, 2008). This phenomenon results in a frost layer on the evaporator leading to an additional thermal resistance and, more importantly, to an increase of pressure drop, affecting the whole system (Song, Xu, Mao, Deng, & Xu, 2017). In the light of these facts, many researches are dedicated to this issue with two main axes, namely the defrost strategies and frost delay. The defrost strategies are mainly active method aiming at removing the frost when a limit quantity of frost is reached (Song, Deng, Dang, Mao, & Wang, 2018). The frost delay consists in applying a specific coating (e.g. hydrophobic coating) to the exchanger to modify the physics at the surface level, having as consequence a time delay on the appearance of the first frost layer (Amer & Wang, 2017). Obviously, combination of both techniques should be

investigated.

Liu, Gou, Wang, and Cheng (2008) and Wang, Kwon, DeVries, and Park (2015) showed experimentally the actual frost delay on coated surfaces. As use of superhydrophobic coatings has shown a real impact on the frost formation process, this paper aims at investigating the impact on the global system level, namely at the heat pump level. An innovative test bench has been built at University of Liège to monitor the performance of a mini exhaust air heat pump in frost conditions, with the possibility of trying different evaporators (with or without coating). This paper presents the test bench in itself and the first experimental results.

2. TEST RIG DESCRIPTION

A dedicated test rig has been built to characterize the frost formation in the heat pump evaporator. The heat pump, as previously mentioned, is a mini exhaust air heat pump. It shows a conventional architecture, as seen in Figure 1, and works with *R134a* fluid.

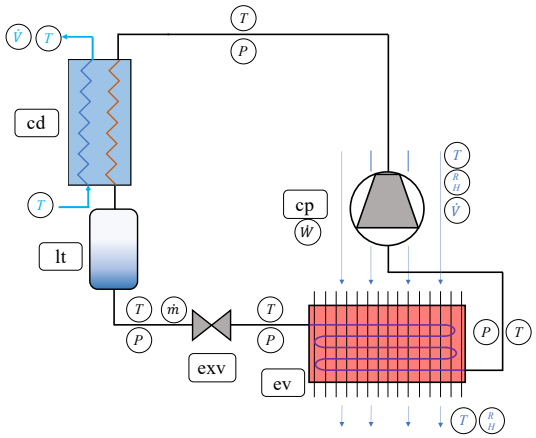

Figure 1: Architecture of the studied heat pump

The condenser is a brazed-plate heat exchanger cooled down with tap water. The exhaust is connected to a liquid tank, ensuring the liquid saturated state of the refrigerant. The liquid mass flow rate is then measured with a Coriolis mass flow-meter before being expanded in an thermostatic expansion valve. The expanded refrigerant is then driven to the evaporator. This exchanger has a tubes and fins configuration. The refrigerant is split in three distinct channels at the inlet and all the fluid is then brought back to a single tube at the outlet. The outer metallic casing of the exchanger has been replaced by transparent polymer, to have a visual control on the frost formation. The refrigerant vapor is then compressed by a constant speed rolling piston compressor of 2300 W.

Table 1: Main components and fluids of the test rig.

Component	Type	Model/Brand	Comment
Working fluid	HFC	R134a	n.a.
Heat source fluid	Air	n.a.	Temperature and humidity controlled
Heat sink fluid	Water	n.a.	Tap water
Compressor (cp)	Rolling piston	Tecumseh RK5512Y	Constant speed
Condenser (cd)	Brazed Plates HEX	Alpha Laval	n.a.
Liquid tank (lt)	Vertical tank	n.a.	Volume = 0.7L
Expension valve(exv)	Orifice	Danfoss	n.a.
Evaporator (ev)	Fins and tubes	EuroCoil	Visual access

The secondary fluid of the evaporator is pressurized air provided at 7 bar, then dried, expanded and cooled down in a cooling coil. The conditions are then around -5°C and 5% relative humidity for a maximum volumetric flow-rate of 240 m^3/h. To obtain the desired air stream conditions, three different lines are controlled (Figure 2 (b)):

- the volumetric flow rate, thanks to a by-pass and a dedicated valve;
- the temperature, with three electrical resistances : two 1.2 kW constant power, and one adjustable 1.5 kW power, tuned with a PID controller;
- the humidity, by injecting high pressure steam in the air flow.

This air flow is injected to an insulated box containing the compressor to cool it down. It then goes in a divergent, in the evaporator and then in a convergent, in order to have the flow as uniform as possible.

The evaporator is not weighted on its own. If frost accrates on the exchanger, the refrigerant condition is going to change. The actual refrigerant mass within the device may then vary, introducing confusion in frost mass measurement. For this reason, the whole set-up is weighted, as the quantity of refrigerant is constant. The heat pump is mounted on a metallic frame and the air connection is made of a flexible aluminum pipe allowing the lowest possible mechanical resistance. The frame is weighted by the mean of a load cell, as shown in Figure 2.

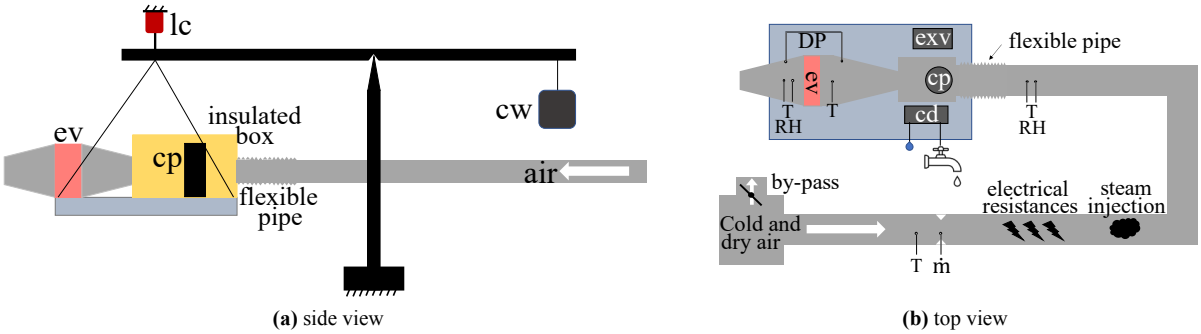

(a) side view **(b)** top view

Figure 2: Set-up scheme of the test bench

Here, a trick is used to unload the sensor. Indeed, the whole test bench set up is around 65 kg. However, the frost quantity weighted is around maximum 1.5 kg. The accuracy of a sensor of a maximum capacity above 65 kg would not be satisfying to measure precise variations under 1 kg. As a consequence, the frame is fixed to a beam, supporting a counter-weight on its opposite side, as shown in Figure 2 (a) and 3. The beam lies on a vertical structure with a mechanical interaction as small as possible. The load cell, firmly clamped, is then connected to the beam (on the HP side). In this way, the sensor range can be much smaller, as the installation weight is counterbalanced. In other words, the sensor does not measure the absolute mass anymore, but only the mass variations. Here, a 2-kg load cell is chosen, affording a 1-g precision.

All the geometrical dimensions of the evaporator are summarized in Table 2

Table 2: Geometry of the evaporator

Characteristic	Value	Units	Characteristic	Value	Units
Width	0.28	m	Exchange area (refrigerant side)	0.36	m^2
Height	0.31	m	Exchange area (air side)	7	m^2
Depth	0.11	m	Distance between tubes (horizontally)	22	mm
Number of rows	12	-	Distance between tubes (vertically)	26	mm
Number of columns	4	-	Tube external diameter	10	mm
Number of fins	140	-	Tube internal diameter	8.5	mm
Fin thickness	0.2	mm			

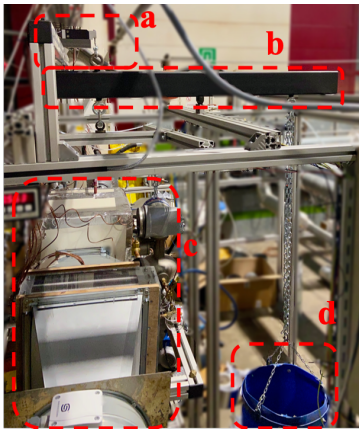

(a) (a) load cell - (b) beam - (c) heat pump - (d) counter wight

(b) beam pivot

Figure 3: Pictures of the test bench

3. CONDENSATES AND FROST MASS MEASUREMENT SYSTEMS

The humidity balance over the evaporator can be evaluated by means of two techniques. On one side there are the humidity sensors combined with air mass flowrate (method *a*). On the other side there is the load cell (method *b*). In this section both techniques are detailed and compared.

$$m_{water,a} = \dot{m}_{air} \cdot (\omega_{su} - \omega_{ex}) \cdot \Delta t \tag{1}$$

$$m_{water,b} = m_{force\ sensor} \tag{2}$$

The sensors involved in those specific measurements are detailed in Table 3. The humidity and force sensors cali-

Table 3: List of sensors

	Measure]	Brand/type	Range	Total error
Load cell	Mass [kg]	Tedea Huntleigh Model 1030	0-2 kg	0.05% m.v.
Air	Temperature [°C]	T type thermocouple	-270 to 370°C	0.5K
	Relative humidity [%]	S+S Regeltechnik KFTF-20-U	0-100%	1.8% (10-90%RH at 25°C) 2% otherwise
	Mass flow rate [kg/s]	Trox + Sensirion SDP1000L05	0-0.15kg/s	5% m.v
Ref	Temperature [°C]	T type thermocouple	-270 to 370°C	0.5K
	Pressure [bar]	General Electric Druk	0-6 bar	0.5% m.v.
	Mass flow rate [kg/s]	Krohne Optimass3300c	0-0.125kg/s	0.1% m.v.

m.v. = measured value

brations are detailed hereafter. For humidity sensors, two calibration steps are driven. First, the relative humidity is corrected regarding reference atmospheric conditions, controlled with saturated aqueous solutions of inorganic salts. Then, because of an absolute humidity deviation with temperature change, measurements are also corrected regarding this point.

Humidity sensors are successively immersed in different sealed bottles. In each bottle, lies a different wetted salt or pure water, setting a known theoretical relative humidity. The solutions used are $KOH_{(aq)}$, $MgCl_{2(aq)}$, $NaCl_{(aq)}$ and pure water, showing at respectively, at 23°C, humidities of 8, 33, 75 and 100%, at equlibrium. The Figure 4 (a) shows the measured relative humidity vales before and after the calibration. The maximal error of 5% is reduced to less then 2%, accuracy of the sensor, at 23°C.

An additional deviation is noticed. The humidity sensors are installed in an air flux showing a constant absolute humidity. Without injecting humidity, the air temperature is artificially increased, thanks to the electrical resistances. The absolute humidity computed based on the relative humidity and temperature measurements is increasing as well, where it should not be. To fix it, a constant humidity is set and the temperature is tuned to different values between 5 and 35°C. The data at 23°C is considered as reliable and a calibration law is deduced. The 23°C temperature is chosen because it is the temperature used for the previous calibration step and it is close to the nominal temperature of the humidity sensor. The results are shown in Figure 4 (b).

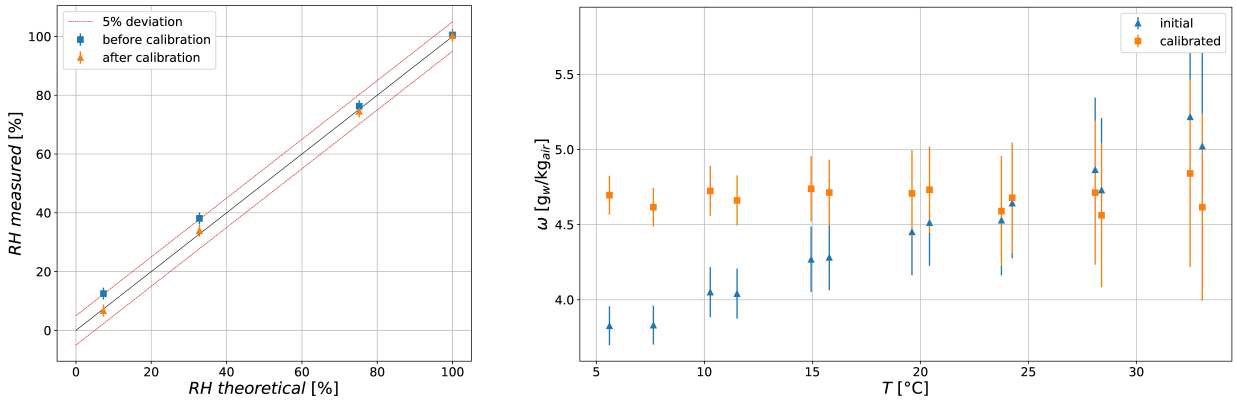

(a) RH calibration - use of moistened salts

(b) Absolute humidity calibration regarding temperature

Figure 4: Humidity calibration

For two reasons, the load cell is calibrated before each test. First because an offset may be observed (not exactly at 0g at the start of the test) and this offset can be different for each test, due to external factors. Then, the two incoming secondary fluids (water at cd and air at the ev) impose a force on the structure. This force depends on the involved flowrates and may have a vertical component, directly impacting the load cell. The procedure is to get the complete setup in steady state, with the compressor off. Then the the evaporator is loaded with different calibrated weights of 50, 200, 500, 1000 and 1500g. Then, a classical calibration law is fitted and implemented in the data post treatment. Finally, the calibration weights are removed, the compressor is turned on and the test begins.

Twenty-eight tests are realized, varying air supply conditions. Four of them, that are representative, are picked up. Their air supply conditions are shown in Table 4.

Table 4: Air conditions for the different tests

Test	$T_{air,su}$ [°C]	ω_{su} [g_{water}/kg_{air}]	$\dot{m}_{air}$ [m^3/h]
blue	24	14	230
orange	24	10	200
green	24	10	150
red	16	6	230

First, the mass accumulation in the evaporator is shown in Figure 5, regarding either the force sensor or humidity balance. The mass accumulation is either liquid condensates, frost accumulation or a combination of both. The ascending part of the curve corresponds to normal operation of the heat pump. At the maximum of the curves, the compressor of the heat pump is stopped but the air flux is still imposed. It leads to a defrost of the evaporator. A part of the water is collected in a bucket through a drilled hole at the bottom of the exchanger. This amount of water is weighted with the complete set up, so it does not imply any variation in either method (a) or (b) measurement technique. The mass decrease is due to water carried away by the air stream or evaporated in the flux.

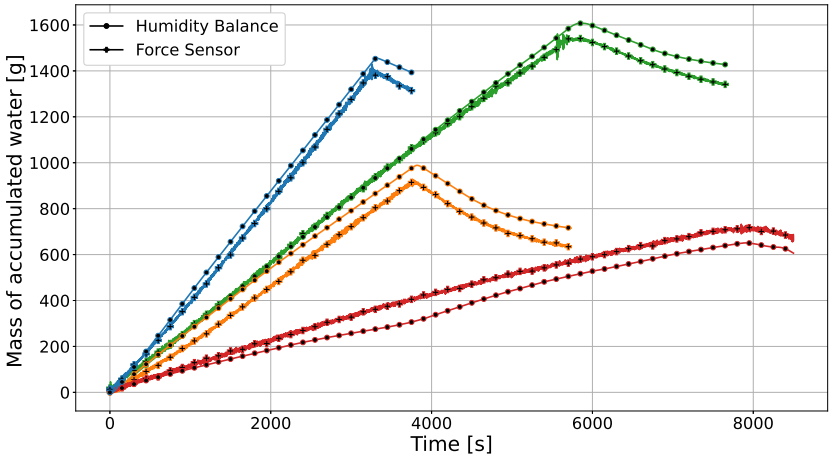

Figure 5: Mass accumulation through time

Then, the measured heat transfer rate is displayed in Figure 6, regarding either the refrigerant side, or the air side using both methods *a* (Eq. 1) and *b* (Eq. 2)) for the latent load. The refrigerant side is taken as the reference, because the sensors involed are much more precise compared to the sensors involved on the air side (especially the mass flow-rate measurement). Only the quasi-steady-state is represented, for clarity reasons.

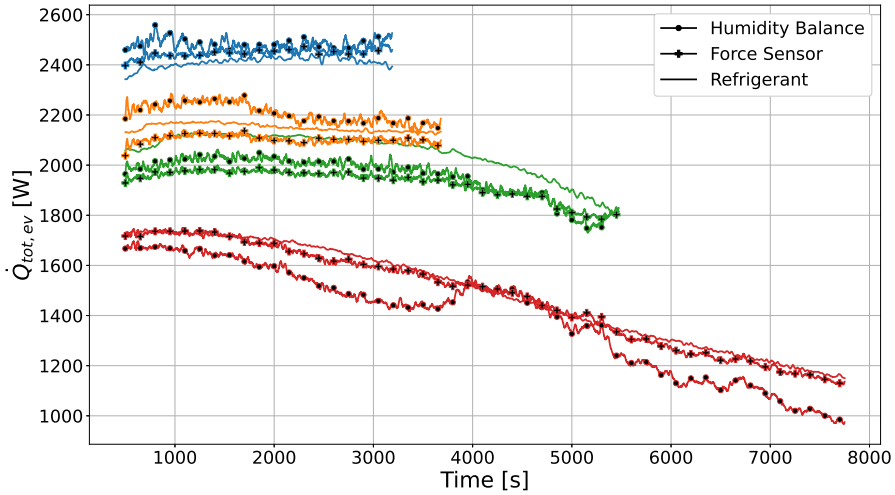

Figure 6: Mass accumulation through time

Despite a slight precision advantage for the load cell use, both techniques show advantages and drawbacks. First, the pros for the method *a* (use of humidity sensors) are exposed:

- Setup simplicity : it is intuitive and no complicated mechanical setup is needed. For the mass measurement using the load cell, the test bench has to be hanged, with a counterweight system. Moreover, the measurement of the air mass flowrate as well as the supply humidity is compulsory anyway.
- No external perturbation can occur, unlike the weighting system which can significantly deviates if anything touches it.

The advantages of the load cell are:

- Stability : looking at Figure 6, the measured power is more stable with load cell, due to the independence of the air flow conditions for the latent load computation.

- Measurement error : with method *a*, a mass increment is measured at each time step with its associated error. On a two hours test, all these arrors may be added, resulting in a global error relatively important. On the other side, the total mass is recorded at each time step. The error is in this case not cumulative.
- Accuracy : besides the error propagation, the amount of water measured relies on either three sensors (2 RH and mass flowrate) for method *a* and only one (load cell) for method *b*. The global accuracy is then better for the load sensor cell

To sum-up, method *b* is more complex to implement but shows better accuracy compared to method *a*. In order to illustrate that, the *red* test is taken on its own and associated uncertainty are analyzed. First, the water mass accumulation is studied. As said before it can be liquid condensates, frost accretion or both. In the case of liquid water, it rolls along fins by gravitational effect. It is then driven to a bucket by means of a small pipe. Everything is weighted.

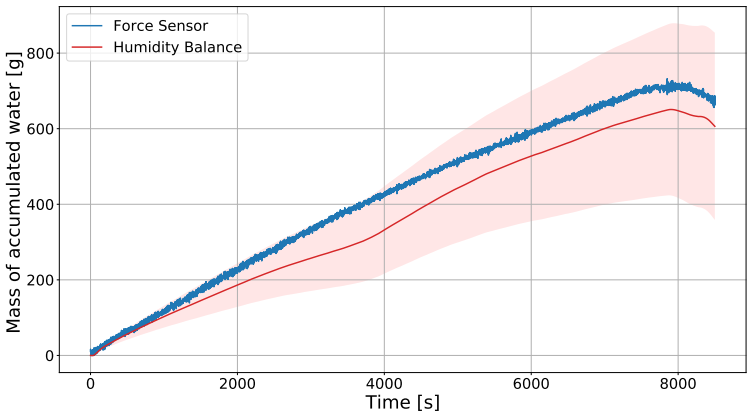

Figure 7: Mass accumulation through time with the uncertainty accumulation

The most striking information in Figure 7 is the dramatic impact of uncertainty accumulation implied by the humidity balance technique. For this precise test, after 2 hours time, a 35% deviation is observed, only staying in sensors deviation range. For each time step, the uncertainty is relatively small implying that the measured power is not that much impacted, as explained after. However, if the goal is to measure the total mass in the exchanger, the method *a* can present major issues. On the other side, the mass measured with the load cells does not show any error in Figure 7. The accurate 2 kg-sensor shows a 1g precision, so the uncertainty is not exposed for clarity reasons. However, the measures do not show a perfectly smooth line. The whole heat pump is weighted and vibrations are induced by the compressor. Yet, those are very limited and does not impact the results.

The Figure 8 shows the total powers measured by means of the different techniques with their associated errors, associated to the *red* test.

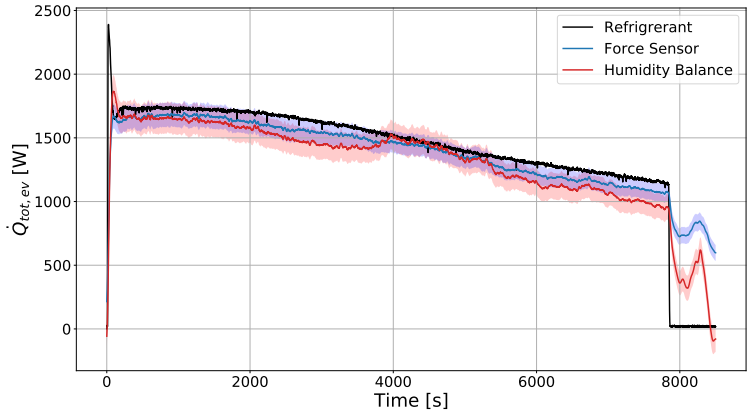

Figure 8: Total power measured with different techniques and associated uncertainties

As previously said, the refrigerant power is taken as the reference. Even if the error is larger for the humidity balance compared to the load cell method, it is still acceptable. To sum up, if the goal is to only predict powers involved in the evaporator, the load cell is not a major ad-on, even if it is slightly more accurate. Nevertheless, if the objective is to characterize the amount of condensates or frost deposition in the exchanger, the load cell is a real improvement.

4. FROST VISUALISATION

Neither the humidity balance nor load cell technique allow to determine if the water accumulation is in liquid or frost state. This is a major issue for studies of this kind of study. To partially counter this point, the outer metallic casing of the evaporator is replaced by transparent polymer material. This allows to have a partial visual control on the exchanger. Indeed, it does not permit to observe what is going on inside the exchanger core, but brings pieces of information.

A *GoPro Hero 5 Black* camera is installed to take snapshots every 30 seconds in 4000x3000 resolution in a linear way. The red and blue tests are picked as examples with a picture at start, after 30 minutes and after 60 minutes.

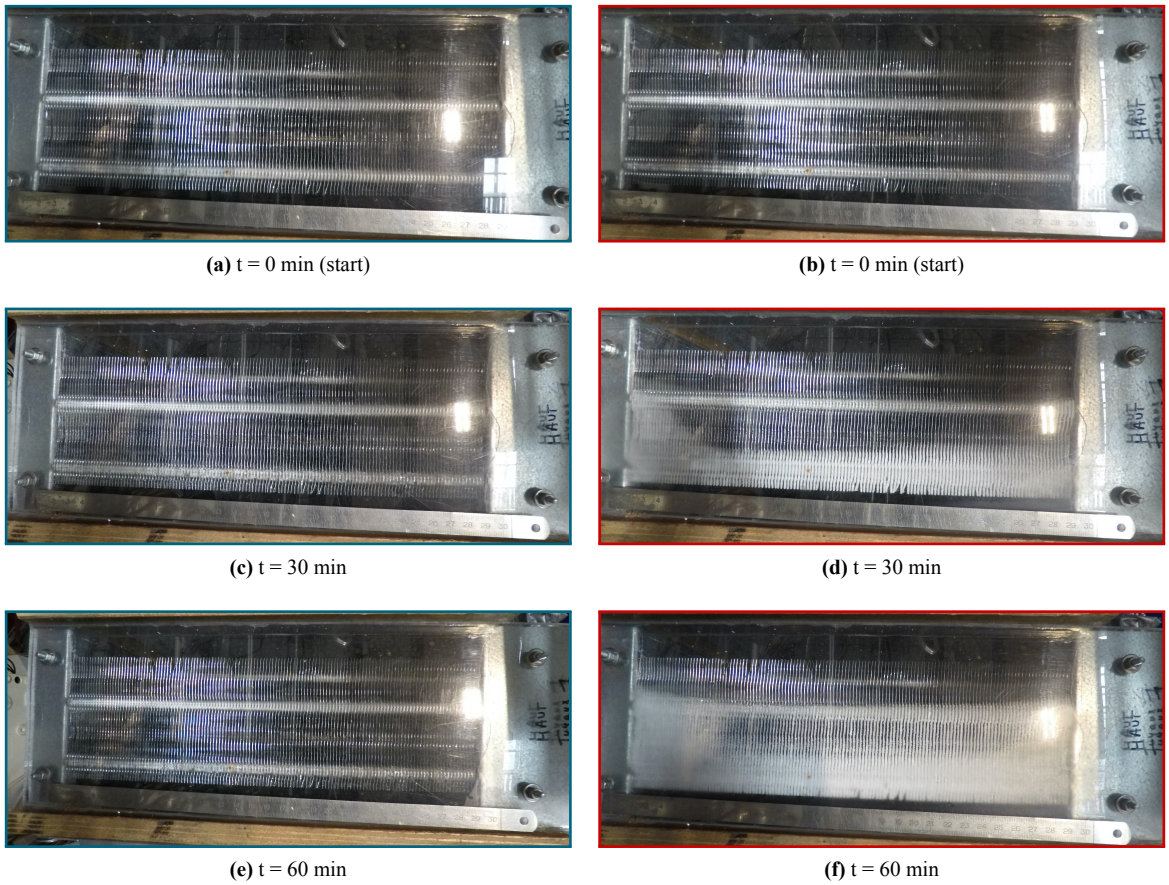

(a) t = 0 min (start) **(b)** t = 0 min (start)

(c) t = 30 min **(d)** t = 30 min

(e) t = 60 min **(f)** t = 60 min

Figure 9: Frost visualisation for blue (left) and red test (right) through time

Even if the blue test in Figure 5 shows a much higher accumulation rate compared to the blue one, Figure 9 reveals no frost accretion, while the blue does. From those simple observations it is easier to deduce if it is liquid water or frost. The two other tests (orange and green) present an intermediate situation with both states. Unfortunately, it does not allow to assert precisely the amount of each phase. This proportion depends on the surface temperature, highly correlated with supply air temperature and flowrate.

5. CONCLUSIONS

This paper present a new test-bench with multiple technique to measure frost mass accumulation and the latent heat transfer in a heat-pump evaporator. The conclusions are the following:

- A test-bench has been designed and implemented to study frost accretion in the evaporator of heat-pump.
- A new weighting system has been installed to increase the accuracy of the measurements. The complete heat pump is hanged to a load cell to avoid the refrigerant distribution issue. A counterweight is built allowing the use of a precise 2-kg load cell.
- The mass weighted is compared to the mass computed by means of humidity balance over the evaporator.
- The load cell shows a better accuracy, especially for the total mass monitoring throughout time (no error accumulation). The difference is smaller while computing the air latent exchanged power.
- A camera records pictures of the exchanger throughout the tests to have a qualitative view of frost deposition.
- This innovative test bench is a new efficient way to experimentally study the frost accretion in refrigeration system.

NOMENCLATURE

$\dot{m}$	mass flow rate	(kg/s)
m	mass	(kg)
P	pressure	(bar)
$\dot{Q}$	heat transfer rate	(W)
RH	relative humidity	(-)
T	temperature	(°C)
$\dot{V}$	volumetric flow rate	(m^3/h)
ω	absolute humidity	(g_{water}/kg_{air})

Subscript

cd	condenser
cp	compressor
cw	counter weight
ev	evaporator
ex	exhaust
exv	expansion valve
lc	load cell
lt	liquid tank
su	supply
tot	total

REFERENCES

Amer, M., & Wang, C.-C. (2017). Review of defrosting methods. *Renewable and Sustainable Energy Reviews*, *73*, 53–74.

Liu, Z., Gou, Y., Wang, J., & Cheng, S. (2008). Frost formation on a super-hydrophobic surface under natural convection conditions. *International Journal of Heat and Mass Transfer*, *51*(25-26), 5975–5982.

Piucco, R. O., Hermes, C. J., Melo, C., & Barbosa Jr, J. R. (2008). A study of frost nucleation on flat surfaces. *Experimental Thermal and Fluid Science*, *32*(8), 1710–1715.

Song, M., Deng, S., Dang, C., Mao, N., & Wang, Z. (2018). Review on improvement for air source heat pump units during frosting and defrosting. *Applied energy*, *211*, 1150–1170.

Song, M., Xu, X., Mao, N., Deng, S., & Xu, Y. (2017). Energy transfer procession in an air source heat pump unit during defrosting. *Applied Energy*, *204*, 679–689.

Wang, Z.-J., Kwon, D.-J., DeVries, K. L., & Park, J.-M. (2015). Frost formation and anti-icing performance of a hydrophobic coating on aluminum. *Experimental Thermal and Fluid Science*, *60*, 132–137.

Xu, Y., Huang, Y., Jiang, N., Song, M., Xie, X., & Xu, X. (2019). Experimental and theoretical study on an air-source heat pump water heater for northern china in cold winter: Effects of environment temperature and switch of operating modes. *Energy and Buildings*, *191*, 164 - 173. Retrieved from `http://www.sciencedirect.com/science/article/pii/S0378778818336909` doi: https://doi.org/10.1016/j.enbuild.2019.03.028

ACKNOWLEDGMENT

Antoine Parthoens would like to thanks the Fund for Scientific Research of Belgium (F.R.S - F.N.R.S) for the financial support - Research fellowship *FC31853*